Amino Acids (2015) 47:483–496
DOI 10.1007/s00726-014-1880-2

ORIGINAL ARTICLE

Phosphoproteomic analysis of the resistant and susceptible genotypes of maize infected with *sugarcane mosaic virus*

Liuji Wu · Shunxi Wang · Jianyu Wu · Zanping Han · Rui Wang · Liancheng Wu · Huimin Zhang · Yanhui Chen · Xiuli Hu

Received: 3 August 2014 / Accepted: 18 November 2014 / Published online: 10 December 2014

Abstract Protein phosphorylation plays a pivotal role in the regulation of many cellular events. No information is yet available, however, on protein phosphorylation in plants in response to virus infection. In this study, we characterized phosphoproteomes of resistant and susceptible genotypes of maize (*Zea mays L.*) in response to Sugarcane mosaic virus (SCMV) infection. Based on isotope tags for relative and absolute quantification technology, TiO_2 enrichment method and LC–MS/MS analysis, we identified 65 and 59 phosphoproteins respectively, whose phosphorylation level regulated significantly in susceptible and resistant plants. Some identified phosphoproteins were shared by both genotypes, suggesting a partial overlapping of the responsive pathways to virus infection. While several phosphoproteins are well-known pathogen response phosphoproteins, virus infection differentially regulates most other phosphoproteins, which has not been reported in literature. Changes in protein phosphorylation status indicated that response to SCMV infection encompass a reformatting of major cellular processes. Our data provide new valuable insights into plant-virus interactions.

Keywords Phosphoproteomic · Maize · Sugarcane mosaic virus · iTRAQ · Plant-virus interactions

Introduction

Potyviridae, which includes approximately, 200 species of economically important plant viruses, causes significant losses in agricultural, pasture, horticultural and ornamental crops. Sugarcane mosaic virus (SCMV), a member of the sugarcane mosaic subgroup of the *Potyviridae*, is an important virus pathogen, especially in maize production, causing serious losses in grain and forage yield in susceptible cultivars (Gan et al. 2010). A high incidence of SCMV and other plant virus co-infection has recently been reported in China (Xu et al. 2008) and other areas, such as Argentina (Perera et al. 2009). It appears that virus mixtures are more virulent than single infections (Xu et al. 2008). In addition, new strains or genomic variants of SCMV continue to be reported in different countries (Perera et al. 2009; Viswanathan et al. 2009; Gao et al. 2011; Padhi and Ramu 2011). These outbreaks indicate that even though SCMV has been long known, it remains an agricultural threat (Wu et al. 2012).

In recent years, genomic and proteomic strategies have been successfully used to analyze plant-pathogen

Electronic supplementary material The online version of this article (doi:10.1007/s00726-014-1880-2) contains supplementary material, which is available to authorized users.

L. Wu · S. Wang · J. Wu · L. Wu · H. Zhang · Y. Chen (✉) · X. Hu (✉)
Henan Agricultural University and Synergetic Innovation Center of Henan Grain Crops, Zhengzhou, China
e-mail: chy9890@163.com

X. Hu
e-mail: xiulihu@126.com

L. Wu · S. Wang · J. Wu · L. Wu · H. Zhang · Y. Chen
Key Laboratory of Physiological Ecology and Genetic Improvement of Food Crops in Henan Province, Zhengzhou, China

Z. Han
College of Agronomy, Henan University of Science and Technology, Luoyang 471003, China

R. Wang
Shanghai Applied Protein Technology Co. Ltd, Shanghai 200233, China

interactions (Margaria et al. 2013). Compared with the study of transcript, the study of proteins has become progressively more important since it is now well-established that proteins are more directly related to function (Pandey and Mann 2000). Although proteomics research in animals is greatly advanced, plant proteomics research is not enough especially in pathogen-host interactions study (Mehta et al. 2008). To identify candidate SCMV resistance proteins and explore molecular mechanisms involved in plant-SCMV interactions, we recently conducted proteomic analyses of leaf samples from resistant and susceptible genotypes of maize infected with SCMV (Wu et al. 2013). Post-translational modifications (PTMs) occurring in host/pathogen proteomes is another important aspect to be analyzed that could take advantage of the potential provided by proteomic tools. PTMs have been found to play an important role in plant defenses against fungal pathogens (Xing and Laroche 2011). However, a study of PTMs has not been taken into account yet in plant–virus interactions (Di Carli et al. 2012).

Phosphorylation is one of the key PTMs regulating protein functions in diverse biological pathways and contexts. Our previous studies identified several protein kinases that are responsive to SCMV infection (Wu et al. 2013), suggesting an important role for phosphorylation events in plant response to virus infection. In this work, based on isotope tags for relative and absolute quantification (iTRAQ) technology and LC–MS/MS analysis, we monitored response to SCMV infection in phosphoproteomes of resistant and susceptible maize genotypes. Phosphoproteins which were found to be significantly regulated were integrated into functional networks to reveal their biological significance in plant-virus interactions. Our data provide new valuable insights into plant-virus interactions.

Materials and methods

Plant materials and virus infection

Maize (*Zea mays* L.) inbred lines Siyi (SCMV-resistant) and Mo17 (SCMV-susceptible) were grown in a containment greenhouse under controlled conditions: 24 °C and a 16-h-light/8-h-dark photoperiod. Maize plants were mechanically inoculated with SCMV at the three-leaf growth stage (14 d after sowing) on their lowest two leaves. The SCMV inoculation mixture was prepared from 100 mg young leaves collected from SCMV-inoculated susceptible Mo17 adult plants displaying typical mosaic symptoms. The infected leaf tissue was homogenized in 1 ml inoculation buffer (0.01 M phosphate buffer, pH 7.0) and mixed with carborundum. Experimental controls were mock-inoculated in parallel using inoculation buffer. Apical leaves were collected from SCMV-inoculated ($Siyi_{SCMV}$, $Mo17_{SCMV}$) and mock-inoculated ($Siyi_{CK}$, $Mo17_{CK}$) plants at 12 d post-inoculation (dpi) and stored at −80 °C until analysis. Each sample consisted of pooled leaves derived from six plants, with three biological replicates collected for each sample.

Phytohormones analysis and chlorophyll measurement

Leaves were collected from SCMV-inoculated plants and mock inoculated plants at 12 days post-inoculation. Leaf tissues were homogenized and extracted in 80 % aqueous methanol according to the method described previously (Escalante-Pérez et al. 2011). Salicylic acid (SA) was assayed using enzyme-linked immunosorbent assay (ELISA) test kits (Hermes Criterion Biotechnology, Canada) according to the manufacturer's instructions. Total chlorophyll (Chl) content was estimated as described by Porra et al. (1989).

Protein digestion

Total proteins were extracted from $Siyi_{SCMV}$, $Siyi_{CK}$, $Mo17_{SCMV}$, and$Mo17_{CK}$ plants using a trichloroacetic acid/acetone procedure (Wu et al. 2013). Briefly, the samples were ground into a powder in liquid nitrogen, transferred into a tube containing 25 ml of trichloroacetic acid/acetone (1:9, v/v) as well as 65 mM dithiothreitol, and then precipitated at −20 °C for 1 h. The samples were centrifuged at 10,000 rpm for 45 min and the supernatants were discarded. 25 ml of acetone was added to the precipitate and the solution was stored at −20 °C for 1 h. The precipitate obtained after centrifugation at 10,000 rpm at 4 °C for 45 min was vacuum-dried, weighted and stored at −80 °C.

After quantification using the bicinchoninic acid method, protein digestion was performed according to the filter-aided sample preparation (FASP) procedure described previously (Wiśniewski et al. 2009). Briefly, 200 μg of proteins for each sample were incorporated into 30 μl STD (4 % SDS, 100 mM DTT and 150 mM Tris–HCl pH 8.0). The detergent, DTT and other low-molecular-weight components were removed using UA buffer (8 M Urea and 150 mM Tris–HCl, pH 8.0) by repeated ultrafiltration (Microcon units, 30 kDa). To block reduced cysteine residues, 100 μl iodoacetamide (0.05 M) in UA buffer was then added and the samples were incubated for 20 min in darkness. Filters were washed three times with 100 μl UA buffer, and then twice with 100 μl DS buffer (50 mM triethyl-ammonium bicarbonate at pH 8.5). Finally, the protein suspensions were digested with 2 μg trypsin (Promega) in 40 μl DS buffer overnight at 37 °C with the resulting peptides collected as a filtrate.

iTRAQ labeling

Peptide content was estimated by UV light spectral density at 280 nm using an extinction coefficient of 1.1 of 0.1 % (g/l) solution that was calculated on the basis of the frequency of tryptophan and tyrosine in vertebrate proteins. The resulting peptide mixture was labeled using 4-plex iTRAQ reagent according to the manufacturer's instructions (Applied Biosystems). For labeling, each iTRAQ reagent was dissolved in 70 μl ethanol and added to the respective peptide mixture. The samples, labeled as 114 ($Mo17_{CK}$), 115($Mo17_{SCMV}$), 116($Siyi_{CK}$), and 117 ($Siyi_{SCMV}$), were multiplexed and vacuum dried. Three independent iTRAQ experiments were performed.

Enrichment of phosphorylated peptides using TiO_2 beads

Enrichment of phosphopeptides was performed according to the procedure reported previously (Larsen et al. 2005). Labeled peptides were mixed, vacuum-concentrated and resuspended in 500 μl loading buffer [2 % glutamic acid, 65 % acetonitrile (ACN), and 2 % TFA]. TiO_2 beads (GL Sciences, Japan) were then added and the mixture was agitated for 40 min. Centrifugation was carried out for 1 min at 5,000 g, and the precipitated beads were set aside. The supernatant was mixed with another set of TiO_2 beads, and centrifugation and bead collection was carried out a second time. Beads from the two centrifugation rounds were combined; they were washed three times with 50 μl washing buffer I (30 % ACN and 3 % TFA) and three times with 50 μl washing buffer II (80 % ACN and 0.3 % TFA) to remove remaining non-adsorbed material. The phosphopeptides were then eluted with 50 μl elution buffer (40 % ACN and 15 % NH_4OH), followed by lyophilization and MS analysis. These peptides were identified/quantified in three replicates.

Mass spectrometry

Five microliters of the phosphopeptide solution was mixed with 15 μl of 0.1 % (v/v) TFA; 10 μl of this mixture was analyzed for nano LC–MS/MS using a Q Exactive mass spectrometer (Thermo Fisher Scientific) equipped with an Easy nLC HPLC (Proxeon Biosystems, now Thermo Fisher Scientific). The peptide mixture was loaded onto a C18-reversed phase column (15 cm long, 75 μm inner diameter, RP-C18 3 μm, packed in-house) in buffer A (0.1 % formic acid) and separated with a linear gradient of buffer B (80 % acetonitrile and 0.1 % formic acid) at a flow rate of 250 nl min^{-1} controlled by IntelliFlow technology over 240 min. The peptides were eluted with a gradient of 0–60 % buffer B from 0 to 200 min, 60 to 100 % buffer B from 200 to 216 min, 100 % buffer B from 216 to 240 min.

For MS analysis, peptides were analyzed in positive ion mode. MS spectra were acquired using a data-dependent top 10 method dynamically choosing the most abundant precursor ions from the survey scan (300–1,800 m/z) for HCD fragmentation. Determination of the target value was based on predictive Automatic Gain Control. Dynamic exclusion duration was 40 s. Survey scans were acquired at a resolution of 70,000 at m/z 200 and resolution for HCD spectra was set to 17,500 at m/z 200. Normalized collision energy was 27 eV and the under fill ratio, which specifies the minimum percentage of the target value likely to be reached at maximum fill time, was defined as 0.1 %. The instrument was run with peptide recognition mode enabled.

Data analysis

MS/MS spectra were searched using Mascot 2.2 (Matrix Science) embedded in Proteome Discoverer 1.4 against the uniprot_poales.fasta (426891 sequences, downloaded Jan 6th, 2013). We use the "decoy database" option in Proteome Discoverer. Proteome Discoverer creates reversed database sequences as decoy database according to the target database submitted. For protein identification, the following options were used: peptide mass tolerance =20 ppm, MS/MS tolerance =0.1 Da, enzyme =trypsin, and missed cleavage =2; carbamidomethyl (C), iTRAQ4/4plex (K) and iTRAQ4/4plex (N-term) were set as fixed modification; oxidation (M) and phosphorylation (S/T/Y) were set as variable modification.

Proteome Discoverer 1.4 was used to extract the peak intensity within 20 ppm of each expected iTRAQ reporter ion from each fragmentation spectrum. Only spectra in which all the expected iTRAQ reporter ions were detected were used for quantification. The phosphopeptide ratios were normalized by dividing by the median ratio of all peptides identified. Phosphorylated peptides were analyzed using Proteome Discoverer 1.4 (Thermo Electron, San Jose, CA) with the score threshold for peptide identification were set at 1 % false discovery rate (FDR) and PhosphoRS site probability cutoffs of 0.75. The phosphorylated sites on the identified peptides were assigned using the PhosphoRS algorithm which calculated the possibility of the phosphorylated site from spectra matched to the identified peptides (Taus et al. 2011). Student's *t* test was used to evaluate the statistical significance, and the false discovery rate (Benjamini-Hochberg) was calculated to correct for multiple comparisons.

Bioinformatics

Molecular functions of identified phosphoproteins were classified according to their gene ontology (GO) annotations combined with their biological function. Subcellular

locations of unique phosphoproteins identified in this study were determined from the UniProt database (http://www.uniprot.org) or predicted using the publicly available program, WolfPsort (http://wolfpsort.org). Protein–protein interactions were analyzed using the publicly available program STRING (http://string-db.org/).

Results

Phenotypic symptoms and physiological parameters of resistant and susceptible maize in response to SCMV infection

To gain insights into changes in protein phosphorylation patterns upon SCMV infection, an inoculation assay was established for resistant maize genotype Siyi and susceptible maize genotype Mo17. Maize plants were periodically examined for phenotypic symptoms which indicated the occurence of disease. At 12 dpi, Mo17 plants showed typical mosaic symptoms, while Siyi plants were symptomless. At this stage, apical leaves of Siyi and Mo17 plants were collected for further analysis. As experimental controls, Siyi and Mo17 plants were mock inoculated with inoculation buffer, and their apical leaves were also collected at the same time. When they were monitored over a prolonged period of time (30 dpi), all SCMV-inoculated Mo17 plants exhibited severe symptoms: the leaves became more yellow and maize plants became severe stunting, whereas Siyi plants remained symptomless.

There is emerging evidence suggesting that a key strategy of plant pathogens is to modify plant hormone levels to promote pathogenicity. Consequently, pathogens have evolved complex repertoires of effector proteins whose functions include modulation of basal phytohormone levels during disease development. SA is one of the important phytohormones which play key roles in mediating disease resistance. We quantified SA after inoculation with SCMV. The results showed that inoculation with SCMV led to SA accumulation at 12 dpi both in Siyi and Mo17 (Fig. 1a). However, total chlorophyll content decreased significantly in Mo17 after inoculation with SCMV, while no obvious change in Siyi (Fig. 1b). These results are consistent with the phenotype symptoms that Mo17 plants showed typical mosaic symptoms, while Siyi plants were symptomless.

Phosphoproteomic changes in resistant and susceptible maize in response to SCMV infection

To study the phosphoproteomic changes in response to SCMV infection in the resistant and susceptible maize, an iTRAQ technique was used. We quantitatively compared the phosphopeptides derived from SCMV-inoculated maize leaves with that derived from mock-inoculated maize leaves. Spectra for all the phosphopeptides, which were found to be significantly regulated, are shown in Supporting Information Figure S1.

In total, 839 phosphopeptides were identified in all three biological replicates. 155 phosphopeptides, corresponding to 124 phosphoproteins, were found to be significantly regulated ($P < 0.05$, ratio ≥ 1.5, FDR < 0.05). Among the 155 phosphopeptides, 76 phosphopeptides (corresponding to 65 phosphoproteins) were significantly changed in the susceptible maize group ($Mo17_{SCMV}/Mo17_{CK}$); of these, 40 phosphopeptides were up-regulated and 36 were down-regulated (Table 1). In the SCMV-resistant maize group ($Siyi_{SCMV}/Siyi_{CK}$), 79 phosphopeptides (corresponding to 59 phosphoproteins) were significantly changed. Of these, 37 were up-regulated and 42 were down-regulated (Table 2). Original data for all the identified phosphopeptides are shown in supplementary Table S1. A Venn diagram illustrating the distribution of differentially regulated phosphopeptides and phosphoproteins is shown in Fig. 2. According to the conventional method of phosphorylation site prediction in identified phosphopeptides (Porra et al. 1989), the distribution of phosphorylation sites was Ser (81.3 %), Thr (16.6 %), and Tyr (2.1 %). In addition, most peptides were singly phosphorylated (supplementary Tables S1 and S2).

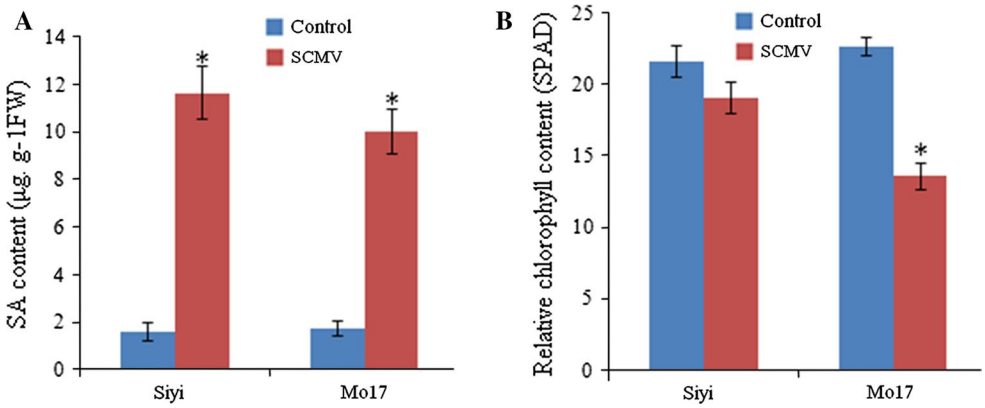

Fig. 1 **a** Salicylic acid (SA) accumulation after *Sugarcane mosaic virus* (SCMV) inoculation. FW, fresh weight. **b** Relative change of chlorophyll content after SCMV inoculation. Data are representative of three independent biological experiments. *Bars* show SE ($n = 3$)

Table 1 Phosphopeptides changed significantly in susceptible maize Mo17 after SCMV infection, as identified by LC–MS/MS

Accession	Sequence	pRS site probabilities	Description	MW (kDa)	pI	Fold change
B6UBN4	AGSGGPDTPVFGDR	S(3): 100.0; T(8): 100.0	Putative uncharacterized protein	62.89	6.61	0.49
B6UBN4	DIFPGSEAASPR	S(6): 100.0; S(10): 100.0	Putative uncharacterized protein	62.89	6.61	0.51
C0P3W9	SAPSTPKRSAPTTPIK	S(1): 79.6	Phosphoenolpyruvatecarboxykinase	73.4	6.93	0.44
C0P3W9	RSAPTTPIK	S(2): 76.7	Phosphoenolpyruvatecarboxykinase	73.4	6.93	0.57
C0P3W9	SAPSTPKRSAPTTPIK	S(1): 76.7	Phosphoenolpyruvatecarboxykinase	73.4	6.93	0.23
C0P3W9	GEAAAQGAPSTPR	S(10): 100.0; T(11): 100.0	Phosphoenolpyruvatecarboxykinase	73.4	6.93	4.1
C0P3W9	GEAAAQGAPSTPR	S(10): 80.0	Phosphoenolpyruvatecarboxykinase	73.4	6.93	0.61
C5YAK8	QVAHAPQELNSPR	S(11): 100.0	Putative uncharacterized protein	27.82	7.34	0.51
C5YAK8	VDSEGAMCGATFK	S(3): 100.0;	Putative uncharacterized protein	27.82	7.34	0.63
B6T6R3	WAGLGTEDDDSDEASP	S(11): 100.0; S(15): 100.0	Calcium ion binding protein	26.87	5.6	5.63
O04014	SKLSAAAK	S(1): 100.0; S(4): 100.0	40S ribosomal protein	28.6	10.71	1.64
O04014	DRRSESLAK	S(4): 100.0; S(6): 100.0	40S ribosomal protein	28.6	10.71	1.72
B6T1H0	SKLSAAVK	S(1): 100.0; S(4): 100.0	40S ribosomal protein	28.63	10.71	1.67
B6T1H0	DRRSESLAK	S(4): 100.0; S(6): 100.0	40S ribosomal protein	28.63	10.71	1.72
C5IHD0	GGMTSHAAVVAR	T(4): 99.2	Cytosolic orthophosphate dikinase	95.66	5.68	6.26
C5IHD0	GGMTSHAXVVAR	T(4): 80.0	Cytosolic orthophosphate dikinase	95.66	5.68	1.79
C5IHD0	NDTDLTASDLK	S(8): 89.7	Cytosolic orthophosphate dikinase	95.66	5.68	1.86
Q9XGW5	LDDASDDEDEEQEDWR	S(5): 100.0	Nitrate reductase	101.46	6.83	0.3
Q9XEI4	QQAVAISPTSK	S(7): 99.3	Unconventional myosin heavy chain	173.35	8.29	0.34
P93804	ATGAFILTASHNPGGPK	T(8): 89.6	Phosphoglucomutase, cytoplasmic	63.06	5.72	0.37
B6T6Z1	GGAGAGEESGSDHDGVLR	S(9): 100.0; S(11): 100.0	Solute carrier family 2, facilitated glucose transporter member 8	53.73	8.29	0.38
B6T9H8	FAPESSGGDGGGSVR	S(5): 89.6	Carboxy-lyase	25.11	5.25	0.38
E3UMH7	LAVAAPAAVQST	T(12): 80.0	Putative growth-regulating factor	20.56	5.17	0.41
F1DJV0	NNLTEGGAESDEEIR	S(10): 80.0	BZIP transcription factor	19.17	10.27	0.42
B6SKY8	NAQVANEASDDDEPESR	S(9): 100.0	Putative uncharacterized protein	14.68	9.55	0.47
B6TSE6	YYDDEDQSDSAAAAAAR	S(8): 98.4; S(10): 98.4	SAM domain family protein	26.01	6.57	0.49
B6TND9	SLEEMSGEAEDSEEEPVGAR	S(12): 98.7	Inorganic phosphate transporter	55.24	7.75	0.5
B6THU8	IPSNDLSHTIR	S(3): 99.2	Sad1-unc84-like protein	48.84	9.01	0.54
B6SJ48	AAAGKEPVSPGTPSSVAAGR	S(9): 99.8; T(12): 95.6	Putative uncharacterized protein	9.21	7.85	0.55
C5WRC6	QATSVEGK	T(3): 100.0; S(4): 100.0	Putative uncharacterized protein	146.98	7.15	0.57
H9B8F8	VHACVGGTSVR	T(8): 98.6	Initiation factor 4A-3-like protein	42.73	6.71	0.58
B6THG9	LNQLNSSGGADDDDEDDE	S(6): 80.0	60S ribosomal protein	34.4	9.32	0.6
Q8RUJ4	GLDIDTIQQNYTV	Y(11):80.0	Plasma membrane H + -transporting ATPase-like protein	5.79	8.57	0.63
B6SUG8	PDSDNESGGPSNAEFSSPR	S(3): 98.8; S(7): 98.8	Nuclear transcription factor Y subunit	22.19	6.39	0.64
C5XA63	LVVHTPLAGTPGSK	T(5): 100.0; T(10): 100.0	Putative uncharacterized protein	18.48	11.19	0.65
B6UHY8	AVSLPSSPNR	S(3): 76.7; S(6): 76.7; S(7): 76.7	ATP binding protein	87.65	6.84	0.29
B6UEQ 3	QLSIHDNR	S(3): 100.0	Dynamin	99.49	9.1	0.25
B4G1F0	SGSLGSNDTYVR	S(3): 100.0	ATP binding protein	41.6	7.94	0.26
B6TJ91	EMSRSPPPPPPR	S(3): 100.0; S(5): 100.0	Splicing factor, arginine/serine-rich	31.3	11.52	0.38
B4FB91	GELALVPQSPDR	S(9): 100.0	Ferritin	19.76	8	6.01
P27347	SEVNDEDDEEGSEEDEDDDE	S(12): 100.0	DNA-binding protein	17.14	5.95	6.01
C5X2Z4	ALIAEGSCGSPR	S(7): 80.0	Glucose-6-phosphate isomerase	67.16	5.47	6.07
B6STN2	PDSDNDSGGPSNAGGELSSPR	S(3): 100.0; S(7): 99.9	Nuclear transcription factor Y subunit	23.23	6.68	5.69
K3Z3Q0	QLSLDQFENESR	S(3): 100.0	Serine/threonine-protein	96.59	6.33	4.15

Table 1 continued

Accession	Sequence	pRS site probabilities	Description	MW (kDa)	pI	Fold change
O81105	NKSFDDDDDFSNK	S(3): 100.0	Leucine-rich repeat transmembrane protein kinase	74.85	6.07	4.43
B4G1K7	VPIEAEMSEDTADDDISSR	S(8): 100.0; T(11): 100.0	Adhesion regulating molecule conserved region family protein	33.75	4.44	1.52
B6SSS0	GLVPVGGGGSSGR	S(10): 80.0	Transposon protein Mutator sub-class	79.18	7.34	1.54
D2KLI5	VVTTPGLIDDSPASPSTPPRPR	S(11): 78.9	Trehalose-6-phosphate synthase	98.03	6.01	1.67
B6TJW9	EVSSDDDFVMPTAQK	S(3): 100.0; S(4): 100.0	Putative uncharacterized protein	29.78	9.14	1.71
B6SPK3	ALQESLNAESPPR	S(10): 99.1	Zinc ion binding protein	57.1	5.83	1.74
P31927	DDIVGLEGASPK	S(10): 100.0	Sucrose-phosphate synthase	118.5	6.67	1.83
H8WFY2	NDTDLTASDLK	T(6): 79.7	Pyruvate orthophosphate dikinase	91.89	5	1.86
Q947C1	SASACSLASGFSFGSAK	S(1): 79.8	Fructose-6-phosphate-2-kinase/ fructose-2, 6-bisphosphatase	81.91	6.02	2.09
B6UE07	VEEKEESDDDMGFSLFD	S(14): 94.1	60S acidic ribosomal protein	7.55	4.36	2.24
C5XMG2	SLGSVSLGAGADPRLAVHVASR	S(1): 75.0	Phosphoglycerate kinase	18.31	11.02	5.65
Q6RXW7	TTSETDFMTEYVVTR	T(9): 99.1; Y(11): 99.1	MAPK	16.07	7.09	5.85
P24993	ATQTVEDSSRPK	T(2): 100.0; T(4): 100.0	Photosystem II reaction center protein	5.48	9.83	2.15
K7UU68	QLGGLPVSGEHLR	S(8): 100.0	Putative phototropic-resoponsive NPH3 family protein	46.82	7.37	2.17
K7VD52	RSPSPPFK	S(2): 100.0; S(4): 100.0	C2H2 zinc-finger family protein	82.13	9.03	1.68
K7V1I2	SPSPPPK	S(1): 100.0; S(3): 100.0	Arginine/serine-rich splicing factor	47.65	12.32	1.59
C0P790	ELRDGEASDDEEEYEAK	S(8): 100.0	Eukaryotic translation initiation factor	39.54	5.48	0.66
B4FJG9	IDYEGTFDSDSGDENNSK	S(9): 96.7; S(11): 96.7	Programmed cell death protein	32.98	7.46	2.29
B4F9D4	GGFDGMYSPGGGLR	Y(7): 80.0	Uncharacterized protein	63.08	6.7	2.32
B6TDL6	KVSGPLDSSVSMK	S(3): 80.0	ubiquitin thiolesterase	51.09	9.38	3.08
C0PHF7	ADSPPSSPQPHVQIGHQR	S(3): 76.7	Uncharacterized protein	58.67	4.96	0.31
O24561	NEAGGIIGTRFESSEVK	T(9): 97.0	Chlorophyll a/b-binding protein	18.56	6.15	1.51
O24561	NEAGGIIGTR	T(9): 100.0	Chlorophyll a/b-binding protein	18.56	6.15	1.58
B4FZ13	VAEGNDVSSTGITK	S(8): 99.5; S(9): 99.5	Uncharacterized protein	62.21	5.24	1.76
K3ZQ10	QANLTGEVLEASSRGR	S(12): 100.0; S(13): 100.0	Uncharacterized protein	154.14	6.73	0.41
K7WFR7	QVADSAEGDEPSL	S(12): 100.0	Putative leucine-rich repeat receptor-like protein kinase family protein	33.31	5.55	0.44
B4FHR5	RVSSGNLVDVAR	S(3): 100.0; S(4): 100.0	RAB, member of RAS oncogene family-like	27.29	9.72	0.47
B6TV58	GHDPQGGMSPPGPGGR	S(9): 100.0	Heterogeneous nuclear ribonucleo-protein A3-like protein	44.72	8.47	0.51
B6U2L0	NVGDDVRSDSEGEDDHED	S(8): 100.0; S(10): 100.0	ASC1-like protein 1	36.62	8.31	0.57
B6TZS3	GEGMGSAVADSGESR	S(14): 97.5	Uncharacterized protein	63.66	9.23	0.58
P05022	GEIVASESR	S(6): 98.9	ATP synthase subunit alpha	48.73	5.9	0.59
B6TH05	NQASPESPGNNQNR	S(7): 99.4	Uncharacterized protein	26.98	7.4	0.6

The distribution of phosphorylated sites in our study was consistent with other plant studies, such as those conducted in *A. thaliana*, rice, soybean and medicago. However, the abundance of tyrosine phosphorylation in maize (2.1 %) in this study is slightly lower than that in *A. thaliana* (4.3 %) (Sugiyama et al. 2008), rice (Nakagami et al. 2010), and higher than that in soybean (0.48 %) (Nguyen et al. 2012) or medicago (1.3 %) (Grimsrud et al. 2010). These variations may be attributed to differences in methodology (e.g. phosphopeptide enrichment and/or LC–MS) or biological system, where each cell type, tissue and organism has a unique phosphoproteome profile. In addition, the absence of virus proteins is likely caused by the low abundance of viral proteins and/or the low degree of phosphorylation.

Gene ontology (GO) analysis

To reveal biological processes and cellular components involved in SCMV stress response in maize, GO analyses were performed using the differentially regulated

phosphoproteins, both up- and down-regulated. As shown in Figs. 3 and 4, these phosphoproteins identified in resistant Siyi and susceptible Mo17 had both overlapping and specific distributions among GO categories. The top three cellular components for identified phosphoproteins were membrane (50.63 %), cytoplasm (46.84 %) and nuclear (36.71 %) in Siyi (Fig. 3a) and cytoplasm (48.68 %), membrane (47.37 %) and nuclear (46.05 %) in Mo17 (Fig. 3b). The top three biological processes for Siyi and Mo17 were identical: metabolic process (51.90 % in Siyi; 56.58 % in Mo17), unknown (30.38 % in Siyi; 28.95 % in Mo17) and response to stimulus (24.05 % in Siyi; 17.11 % in Mo17) (Fig. 4a). When analyzed on the basis of molecular functions, the top three categories for the identified phosphoproteins in resistant Siyi (Fig. 4b) were catalytic activity (35.44 %), nucleotide binding (26.58 %) and unknown (22.78 %), and in susceptible Mo17 (Fig. 4b) were catalytic activity (36.84 %), unknown (30.26 %) and protein binding (18.42 %).

In regard to stress/defence responses, GO categories "response to stimulus" and "defense response" were over-represented in both the resistant Siyi and susceptible Mo17 (Fig. 4). However, most phosphoproteins categorized under "response to stimulus" and "defense response" were down-regulated in the susceptible Mo17. In contrast, most phosphoproteins associated with these biological processes were up-regulated in resistant maize. These results indicate that diversified cellular processes and cellular components are involved in virus stress response, and that these two different maize genotypes—one resistant to SCMV infection, and the other susceptible to SCMV infection, contained different sets of virus stress response phosphoproteins. However, it should be noted that one protein could be grouped into more than one GO category sometimes. Therefore, the total percentage in each category is over 100 % when added together.

Protein–protein interactions analysis

Proteins in a living cell do not act as single entities, but rather work together in the context of networks. It has been reported that physical interactions between proteins can be regulated by phosphorylation (Lasonder et al. 2012). To better elucidate virus infection processes regulated by phosphorylation, a protein–protein interaction network (Fig. 5) was constructed based on the phosphoproteins whose phosphorylation level were significantly changed after SCMV infection using the STRING system (http://string-db.org).

Discussion

In the current study, we identified 65 phosphoproteins (76 phosphopeptides) whose phosphorylation level changed significantly in response to SCMV infection in susceptible maize Mo17 and 59 phosphoproteins (79 phosphopeptides) in resistant maize Siyi. Twenty-five of these phosphoproteins were regulated significantly in both Mo17 and Siyi, with consistent or inconsistent phosphorylation patterns. While several phosphoproteins are well-known pathogen response phosphoproteins, virus stress differentially regulation of the majority of the other proteins has not been reported previously. Based on evidences from the literature, some phosphoproteins were previously reported to be regulated following abiotic stress in other plants. Our research also suggests a role for their differential phosphorylation status in response to biotic stress. These findings are in good agreement with recent reports suggesting that mechanisms by which plants respond to different stresses (abiotic and biotic) are not independent, but instead participate in crosstalk with one another and share several biochemical networks at least partially overlapped (Cerny et al. 2011; Huang et al. 2011; Atkinson and Urwin 2012).

The effect of SCMV infection on stress and defense response

Phosphorylation changes in proteins involved in stress and defense response accounted for a major part of the whole detected variations. Within this group, MAPKs are the last component of a conserved three-kinase module of MAPK cascades (Hamel et al. 2006). In plants, MAPK signaling has been implicated in abiotic and biotic stress situations such as pathogen infection, wounding, low temperature, drought, hyper- and hypo-osmolarity, high salinity, touch, and reactive oxygen species (ROS) (Zwerger and Hirt 2001). In our study, phosphorylation of MAPK was up-regulated (5.8-fold) in Mo17 after SCMV infection, confirming the phosphorylation events involved in regulating plant-virus interactions.

Incompatible plant-pathogen interactions usually induce hypersensitive response and host defense mechanisms (Bent 1996). The hypersensitive response, characterized by rapid, localized cell death of plant cells directly in contact with or close to the site of pathogen attack, is a form of programmed cell death (Morel and Dangl 1997). In this study, the phosphorylation level of a programmed cell death protein was up-regulated (2.2-fold) in response to SCMV infection in Mo17, suggesting that the increased level may also function inhibitory.

Iron is an essential element for most living organisms, and pathogens are likely to compete with their hosts for the acquisition of this element. Interestingly, the phosphorylation levels of three proteins involved in iron homeostasis were significantly changed by SCMV infection in Siyi. These phosphoproteins include ferredoxin, ferritin and ferric reductase-like transmembrane component. In higher

Table 2 Phosphoproteins changed significantly in resistant maize Siyi after SCMV infection, as identified by LC–MS/MS

Accession	Sequence	pRS site probabilities	Description	MW (kDa)	pI	Fold change
C5IHD0	GGMTSHAXVVAR	S(5): 80.0	Cytosolic orthophosphate dikinase	95.66	5.68	0.27
C5IHD0	GGMTSHAAVVAR	T(4): 99.2	Cytosolic orthophosphate dikinase	95.66	5.68	0.45
C5IHD0	GGMTSHAAVVAR	T(4): 99.1	Cytosolic orthophosphate dikinase	95.66	5.68	0.56
P31927	EATEDLAEDLSEGEK	S(11): 100.0	Sucrose-phosphate synthase	118.5	6.67	0.29
P31927	DDIVGLEGASPK	S(10): 100.0	Sucrose-phosphate synthase	118.5	6.67	0.47
P31927	GAGGGGGGGDPRSPTK	S(13): 98.5	Sucrose-phosphate synthase	118.5	6.67	0.47
P31927	NFSDLTVWSDDNK	S(3): 100.0	Sucrose-phosphate synthase	118.5	6.67	0.47
C0P3W9	SAPSTPKRSAPTTPIK	S(1): 76.7	Phosphoenolpyruvatecarboxykinase	73.4	6.93	0.3
C0P3W9	SAPTTPIK	S(1): 76.7	Phosphoenolpyruvatecarboxykinase	73.4	6.93	0.4
C0P3W9	SAPTTPIK	S(1): 100.0	Phosphoenolpyruvatecarboxykinase	73.4	6.93	0.48
C0P3W9	AQTIDELHSLQR	S(9): 100.0	Phosphoenolpyruvatecarboxykinase	73.4	6.93	0.56
C0P3W9	RSAPTTPIK	S(2): 76.7	Phosphoenolpyruvatecarboxykinase	73.4	6.93	0.65
C0P3W9	GGAHSPFAVAISEEER	S(5): 100.0	Phosphoenolpyruvatecarboxykinase	73.4	6.93	2.95
H8WFY2	GGMTSHAAVVAR	T(4): 99.2	Pyruvate orthophosphate dikinase	91.89	5	0.45
H8WFY2	GGMTSHAAVVAR	T(4): 99.1	Pyruvate orthophosphate dikinase	91.89	5	0.56
B6UBN4	LFSPESSPK	S(3): 98.6; S(6): 98.6	Putative uncharacterized protein	62.89	6.61	0.5
B6UBN4	AGSGGPDTPVFGDR	S(3): 100.0; T(8): 100.0	Putative uncharacterized protein	62.89	6.61	0.58
B6SUQ3	YASVSPPR	S(3): 100.0; S(5): 100.0	Putative uncharacterized protein	35.76	5.78	0.54
B6SUQ3	RTPPDSPPR	T(2): 100.0; S(6): 100.0	Putative uncharacterized protein	35.76	5.78	0.59
C5WRC6	GQSALGSALGLISR	S(3): 76.7	Putative uncharacterized protein	146.98	7.15	0.58
C5WRC6	QATSVEGK	T(3): 100.0; S(4): 100.0	Putative uncharacterized protein	146.98	7.15	0.63
B6T1H0	DRRSESLAK	S(4): 100.0; S(6): 100.0	40S ribosomal protein	28.63	10.71	1.64
B6T1H0	SKLSAAVK	S(1): 100.0; S(4): 100.0	40S ribosomal protein	28.63	10.71	1.79
O04014	DRRSESLAK	S(4): 100.0; S(6): 100.0	40S ribosomal protein	28.6	10.71	1.64
O04014	SKLSAAAK	S(1): 100.0; S(4): 100.0	40S ribosomal protein	28.6	10.71	1.76
C5YAK8	VDSEGAMCGATFK	S(3): 100.0	Putative uncharacterized protein	27.82	7.34	1.54
C5YAK8	QVAHAPQELNSPR	S(11): 100.0	Putative uncharacterized protein	27.82	7.34	2.02
C5YAK8	VDSEGAMCGATFK	S(3): 100.0	Putative uncharacterized protein	27.82	7.34	2.32
B6SW74	LEDDKWDASQSPR	S(9): 80.0	Ferric reductase-like transmembrane component	83.94	7.97	0.46
C5WNL2	WEQSNDDSAANNSGGEGGTGGR	S(13): 98.5	Putative uncharacterized protein	77.11	7.09	0.55
C5X906	QAALVLNASR	S(9): 100.0	Putative uncharacterized protein	5.08	10.58	0.61
B6TAW2	NIDNMDGNDGSSPDSSPNR	S(11): 100.0; S(12): 100.0	Chaperone protein	43.6	5.54	0.37
B6SS20	NRLSENTELQSAK	S(4): 80.0	Phototropin	100.75	7.58	0.65
C5XA63	LVVHTPLAGTPGSK	T(5): 100.0; T(10): 100.0	Putative uncharacterized protein	18.48	11.19	0.65
P27347	SEVNDEDDEEGSEEDEDDDE	S(12): 100.0	DNA-binding protein	17.14	5.95	0.66
A2TJU6	VGSAADWSNQF	S(3): 99.9	Aluminum-induced protein-like protein	26.72	6.52	1.54
C5YUE1	ASFAADSGDESGPGEPSSSR	S(7): 100.0; S(11): 100.0	O-acyltransferase	57.82	8.91	1.55
C5WT62	TLYGVVDDGSSDEDESTSK	S(10): 100.0; S(11): 100.0	Putative uncharacterized protein	180.73	8.24	1.55
Q9ATM4	ALGSFRSNA	S(4): 100.0; S(7): 100.0	Aquaporin	30.78	8.13	1.55
P29036	GELALVPQSPDK	S(9): 100.0	Ferritin	28.01	5.81	1.55
B6T8U5	LSAAQAVAAIQPTSPR	T(13): 80.0	ER6 protein	27.72	5.64	1.56
B6UEQ 3	QLSIHDNR	S(3): 100.0	Dynamin	99.49	9.1	1.56
B4G1K7	VPIEAEMSEDTADDDISSR	S(8): 100.0; T(11): 100.0	Adhesion regulating molecule conserved region family protein	33.75	4.44	1.6
B6THU8	IPSNDLSHTIR	S(3): 99.2	Sad1-unc84-like protein	48.84	9.01	1.64
B4FAA8	LAADNAGDTEASPR	S(12): 99.0	Transmembrane protein	34.81	7.87	1.65
B6SRU0	LDQSSPASSPAAVK	S(4): 80.0	Protein binding protein	74.36	9.66	1.78
B6TKR8	DAEGSDGEEEVDQEAEK	S(5): 100.0	NF-180	18.09	4.26	1.79
B4FQK5	SFDELSDDDDVYEDSD	S(6): 100.0; S(15): 100.0	Eukaryotic peptide chain release factor subunit	49.16	5.52	1.87
B4FF90	VVAQHEEREEEDSD	S(13): 100.0	Phosducin-like protein	28.32	4.88	1.88

Table 2 continued

Accession	Sequence	pRS site probabilities	Description	MW (kDa)	pI	Fold change
B6U8S9	LGLSGLGGSPR	S(9): 100.0	Putative uncharacterized protein	27.94	8.09	1.9
Q6JN48	VDNVTYEEDQRSDVVPSPR	S(12): 96.7; S(17): 96.7	Ethylene insensitive	136.56	6.37	1.96
B6SKY8	NAQVANEASDDDEPESR	S(9): 100.0	Putative uncharacterized protein	14.68	9.55	2
B4FB91	GELALVPQSPDR	S(9): 100.0	Ferritin	19.76	8	2.04
B4FI86	TPVEQEMADAPTASA	T(12): 80.0	Proteasome subunit beta type	30.13	5.67	2.12
B6UH65	STGTAATGGSDAGLEEGK	T(4): 76.5	Zinc transporter	37.69	6.84	2.3
B6TBM4	LSVAAQAAAIQPSSPR	S(14): 80.0	USP family protein	27.62	4.88	2.31
B6TND9	SLEEMSGEAEDSEEEPVGAR	S(12): 99.1	Inorganic phosphate transporter	55.24	7.75	2.32
Q9SLP6	LIYTNDAGEIVK	Y(3): 80.0	Ferredoxin	39.3	8.32	2.98
F1DJV0	NNLTEGGAESDEEIR	T(4):80.0	BZIP transcription factor	19.17	10.27	3.87
D2KLI5	VVTTPGLIDDSPASPSTPPRPR	T(17): 78.9	Trehalose-6-phosphate synthase	98.03	6.01	4.07
B6T6R3	WAGLGTEDDDSDEASP	S(11): 100.0; S(15): 100.0	Calcium ion binding protein	26.87	5.6	5.52
Q6RXW7	TTSETDFMTEYVVTR	T(9): 99.1; Y(11): 99.1	MAPK	16.07	7.09	5.75
C0PE12	AQIATVR	T(5): 100.0	Uncharacterized protein	51.82	8.37	0.35
C0PE12	AQAEEETLASER	T(7): 100.0	Uncharacterized protein	51.82	8.37	0.6
K7V7B2	TIKESMDELNSQR	T(1): 100.0; S(5): 100.0	Serine/threonine-protein kinase	56.29	9.13	0.38
K7V7B2	TIKESMDELNSQR	T(1): 100.0; S(5): 100.0	Serine/threonine-protein kinase	56.29	9.13	0.48
B6SYC2	EAEAAAEAESAAGEQK	S(10): 100.0	Uncharacterized protein	69.21	9.48	0.49
P24993	ATQTVEDSSRPK	T(2): 100.0	Photosystem II reaction center protein	5.48	9.83	0.53
B6TRM8	AQELPLKTPENSPK	T(8): 100.0; S(12): 100.0	RanBP1 domain containing protein	47.32	4.81	0.56
K3ZQ10	QANLTGEVLEASSRGR	S(12): 100.0; S(13): 100.0	Uncharacterized protein	154.14	6.73	0.57
C0P9I0	SSSPQVSSLK	S(3): 99.3	Uncharacterized protein	66.63	4.92	0.58
B6TB81	GRYSPAYSPPR	Y(3): 99.6; S(4): 93.5	SR repressor protein	30.47	11.22	0.65
B4FWN6	RPAAPAGSDDDDDGGGG ALAAAR	S(8): 100.0	Putative RING zinc finger domain superfamily protein	36.11	7.77	1.52
C0P5V9	GPVILISDEDED	S(7): 100.0	Uncharacterized protein	12.32	8.5	1.62
C0P594	KADDGEESLDEDDLT	S(8): 100.0	Uncharacterized protein	25.77	4.84	1.65
B4FQI5	NAVEDDAESDDEEVPEGR	S(9): 100.0	Uncharacterized protein	28.26	5.01	1.77
C0P790	ELRDGEASDDEEEYEAK	S(8): 100.0	Eukaryotic translation initiation factor	39.54	5.48	1.83
C0PFZ2	GFVPFVPGSPVER	S(9): 100.0	Sodium/hydrogen exchanger	32.18	9.7	2.23
K7UU68	QLGGLPVSGEHLR	S(8): 100.0	Putative phototropic-resoponsive NPH3 family protein	46.82	7.37	5.18

plants, ferredoxin is encoded by a small gene family whose members display tissue-specific expression and perform specified tasks in different organs (Hanke et al. 2004). In fact, the level of ferredoxin has been found to be related to plant resistance to stress conditions (Huang et al. 2004). In our study, the phosphorylation levels of ferredoxin was up-regulated in resistant maize Siyi, but was unchanged in susceptible Mo17. It is indicated that ferredoxin may plays a positive roles in maize for the resistance to SCMV infection. In addition, the phosphorylation level of ferric reductase-like transmembrane component was down-regulated in resistant Siyi after SCMV infection. Mutants in ferric reductase-like transmembrane component are deficient in ferric iron uptake (Roman et al. 1993). Ferritin, one of the major proteins of iron metabolism, may constitute a missing link in the regulatory loop between iron and ROS (Arosio and Levi 2002). Microarray data have shown that iron deficiency directly affects expression levels of ROS-related genes (O'Rourke et al. 2007). Therefore, our results suggest a possible resistance model in which SCMV infection induces iron homeostasis activity, thereby leading to decreased ROS expression. Lowered ROS expression levels then activate the expression of plant defense-related proteins and strengthen mechanical barriers.

The effect of SCMV infection on metabolic process

Pathogenic infections often induce some common physiological alterations in plants, the most important being metabolic perturbations (van Loon 1987). Most of the 65 significantly regulated phosphoproteins identified in susceptible Mo17 after SCMV infection were involved in metabolic processes. One of these metabolic processes is photosynthesis, which occurs mainly within leaves. Several studies have revealed that virus-infected plants are generally characterized by a decreased photosynthetic rate, suggesting

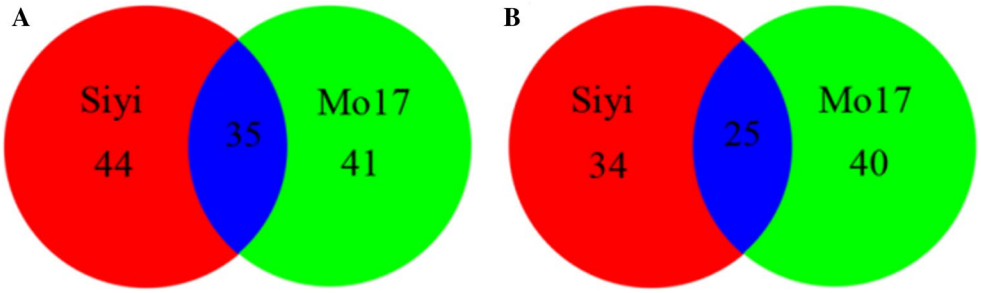

Fig. 2 Venn diagram analyses of differentially regulated phosphopeptides and phosphoproteins in resistant and susceptible maize plants in response to SCMV infection. **a** Venn diagram of differentially regulated phosphopeptides; **b** Venn diagram of differentially regulated phosphoproteins

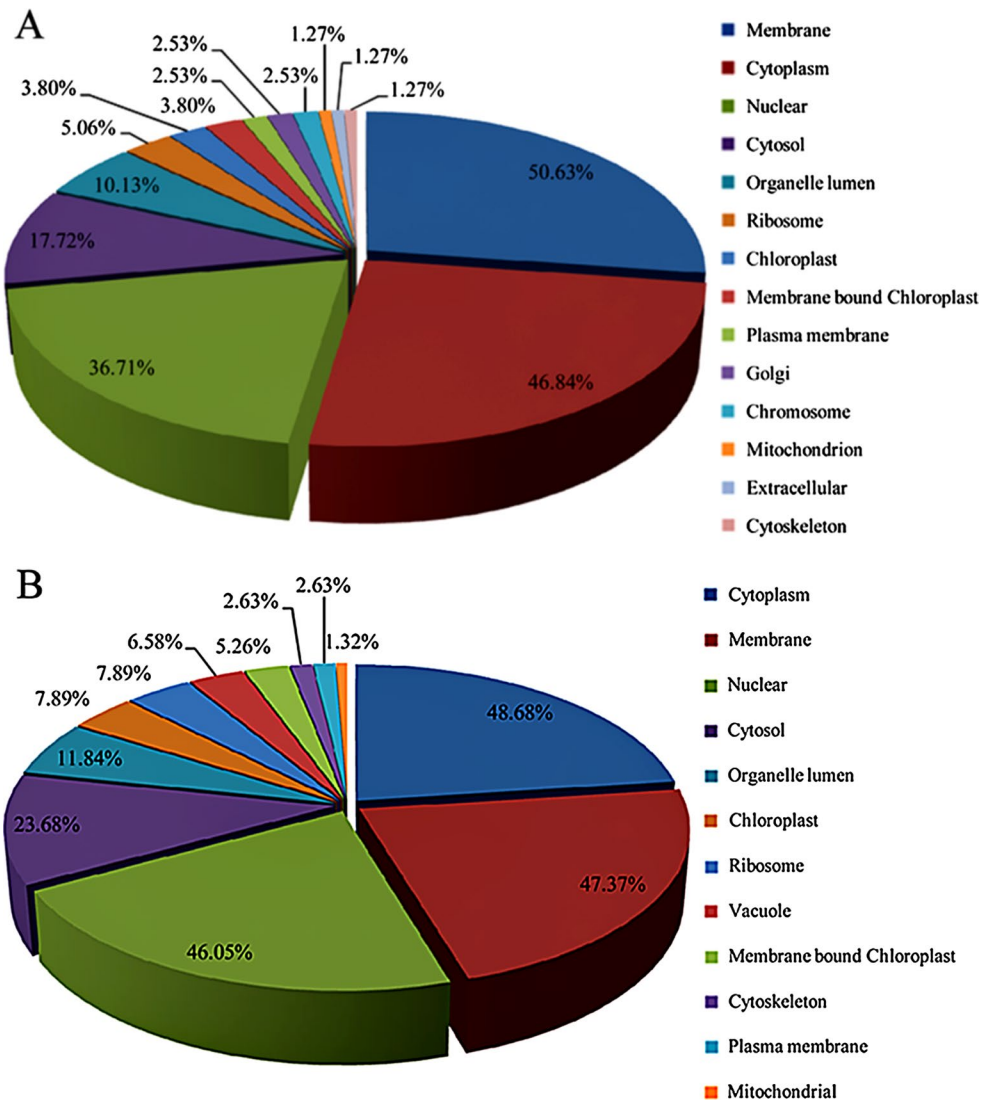

Fig. 3 Gene Ontology distribution of differentially regulated phosphoproteins. **a** Phosphoprotein distribution based on cellular localization in sample group $Siyi_{SCMV}/Siyi_{CK}$; **b** phosphoprotein distribution based on cellular localization in sample group $Mo17_{SCMV}/Mo17_{CK}$

that photosynthesis is one of the major repressed activities during host defense responses (Scharte et al. 2005). In this study, however, the phosphorylation levels of most photosynthesis-related proteins were up-regulated in Mo17 but down- regulated in Siyi (Tables 1, 2). This result indicates that photosynthetic ability is different between resistant Siyi and susceptible Mo17.

Another class of phosphoproteins involved in metabolic processes is ribosomal proteins. Phosphorylation levels of three ribosomal proteins were differentially regulated in Mo17 after SCMV infection, with 40S ribosomal protein and 60S acidic ribosomal protein up-regulated, and 60S ribosomal protein down-regulated. A comparative 2-D gel analysis of proteins from normal and mutant plants,

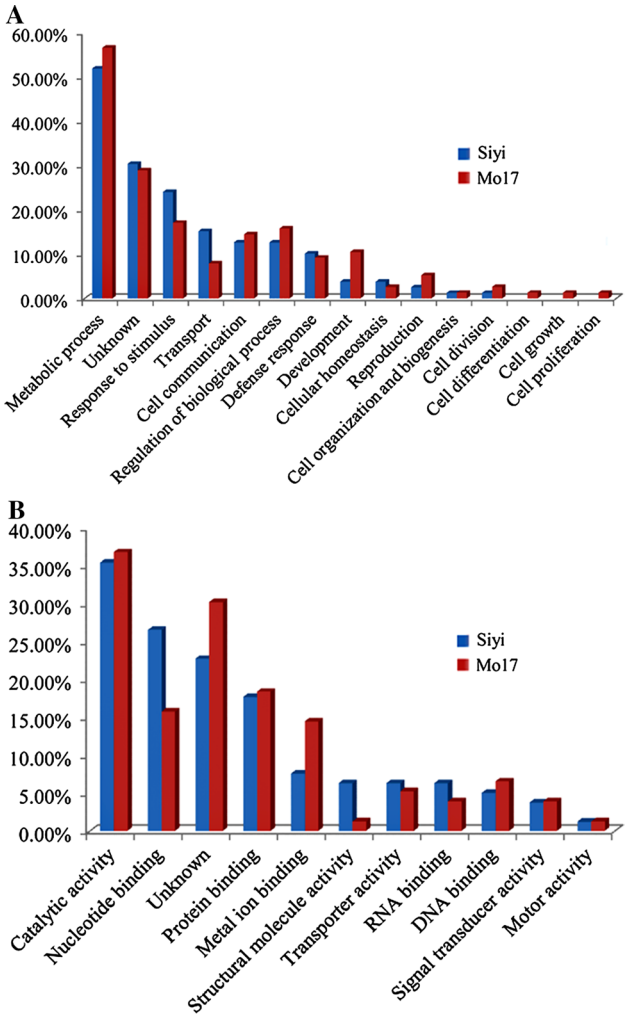

Fig. 4 **a** Phosphoprotein distribution based on biological process; **b** phosphoprotein distribution based on molecular function. Percentage distribution of differentially regulated proteins was used

combined with other biochemical analyses, identified seven target proteins as being phosphorylated and one of these proteins is 60S ribosomal protein (Shin et al. 2007). In addition, 60S ribosomal protein and 60S acidic ribosomal protein have been reported to perform functions related to plant defense: 60S ribosomal protein has been identified as an early-changed component upon elicitor treatments in *A. thaliana* membrane phosphoproteome (Benschop et al. 2007), whereas 60S acidic ribosomal protein acts as an *A. thaliana* determinant of *Peronospora parasitica* specific recognition through a gene-for-gene mechanism (Sinapidou et al. 2004). In addition, 40S ribosomal protein, an MPK3 substrate on microarray analysis, was also found to be phosphorylated in *A. thaliana.* (Carroll et al. 2008).

Most of the phosphoproteins regulated significantly in resistant maize Siyi after SCMV infection were also involved in metabolic processes. Sucrose is the major transport carbohydrate in many plant species and, as such, forms the interface between carbon assimilation in source tissue and carbon utilization in sink tissue (Baxter et al. 2003). In this study, the phosphorylation levels of four sucrose phosphate synthase isoforms were all down-regulated in Siyi after SCMV infection. Sucrose-phosphate synthase is subject to a complex system of regulation involving post-translational modulation of activity via protein phosphorylation and direct control via metabolic effectors (Huber and Huber 1996). In addition, tomato plants expressing a sucrose phosphate synthase gene under the control of the CaMV35S promoter have been found to have increased biomass compared with controls (Laporte et al. 2001).

The phosphorylation level of a photosynthesis-related phosphoprotein, phototropin, was also down-regulated in Siyi after SCMV infection. Phototropins are serine/threonine kinases activated by auto-phosphorylation that are involved in optimization of photosynthetic efficiency (Christie et al. 2007). Phosphorylated phototropin stimulates stomatal opening, and a smaller pool of phosphorylated phototropin is expected to lead to stomatal closure and a decreased CO_2 uptake, leading to inhibition of photosynthesis (Stulemeijer et al. 2009). Pathogens can trigger stomatal closure through pathogen-associated molecular patterns, preventing penetration through these pores. Hence, the stomata can be considered part of the plant innate immune response (Gudesblat et al. 2009). Consequently, down-regulation of the phosphorylation levels of phototropins is correlated with stomatal closure and may trigger the innate immune response of resistant maize Siyi to SCMV infection.

The effect of SCMV infection on other functional groups

Among these identified phosphoproteins, several phosphoproteins involved in a variety of DNA/RNA processes were found to be significantly regulated in maize Mo17, including BZIP transcription factors, eukaryotic translation initiation factor and serine/arginine rich splicing factors. These results suggest that transcription and translation are major targets for regulatory phosphorylation during plant-virus interactions. This would certainly be consistent with the large cellular changes associated with the maize infection process. Aquaporins are ubiquitously present in living organisms including plants. These are channel proteins involved in mediating transport across membranes of water, small neutral solutes, and occasionally ions in response to abiotic stresses (Maurel et al. 2007). Phosphorylated serine residues have previously been reported in the N- and C-terminal tails of various plant aquaporins (Daniel and Yeager 2005). Prak et al. have provided evidence for abiotic stress-induced quantitative changes in aquaporin phosphorylation

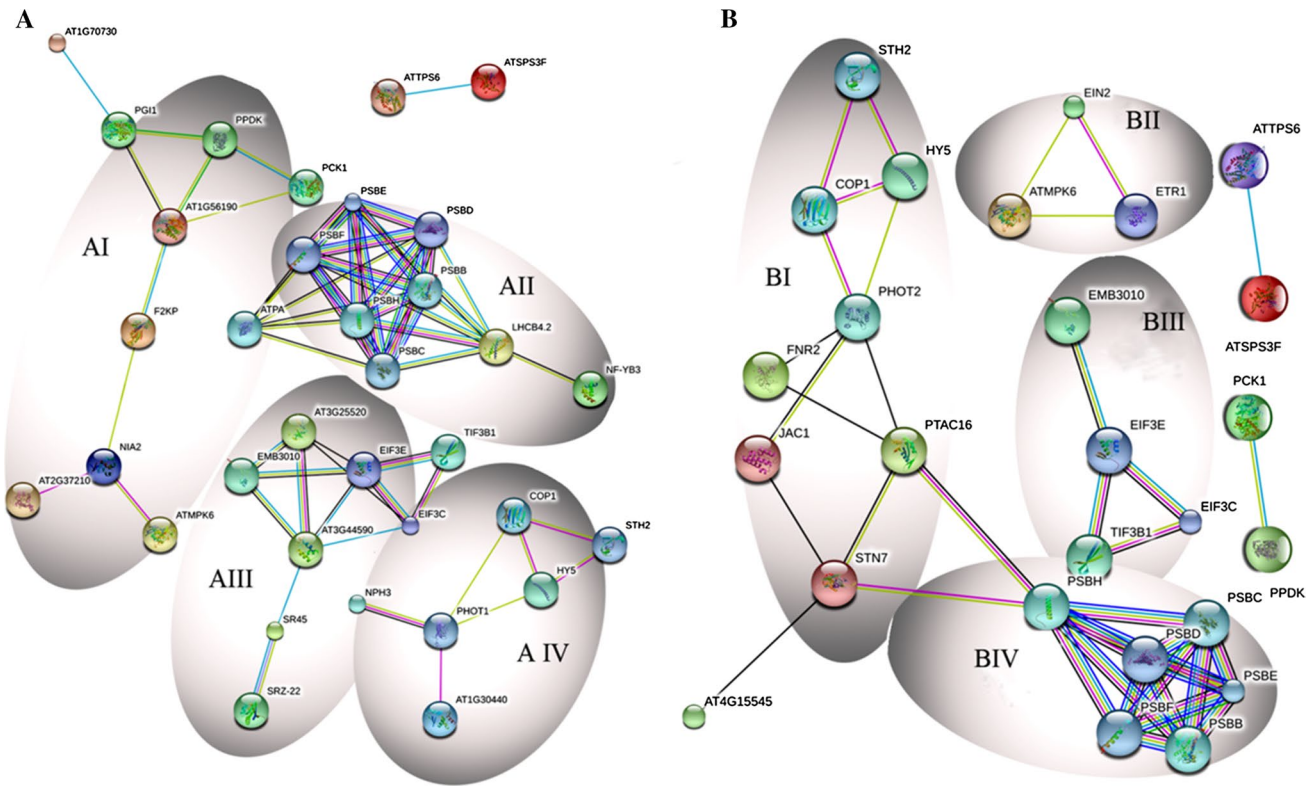

Fig. 5 Interaction network of identified phosphoproteins. Network mapping was performed using the STRING system. **a** Network derived from analysis of differentially regulated phosphoproteins in sample group $Mo17_{SCMV}/Mo17_{CK}$. Four major clusters derived from the associations of the phosphoproteins were marked with AI, AII, AIII and AIV. **b** Network analyzed from differentially regulated phosphoproteins in sample group $Siyi_{SCMV}/Siyi_{CK}$. Four major clusters derived from the associations of the phosphoproteins were marked with BI, BII, BIII, BIV. Different line colors represent types of evidence for association: *green line* neighborhood evidence, *red line* fusion evidence, *purple line* experimental evidence,*light blue line* database evidence, *black line* coexpression evidence, *blue line* co-occurrence evidence, and *yellow line* text-mining evidence. Phosphoproteins without interactions are not shown (color figure online)

and its link with sub-cellular localization (Prak et al. 2008). In the present study, the phosphorylation level of aquaporin was up-regulated by SCMV infection, indicating that aquaporin phosphorylation can also be induced by biotic stress.

Finally, several phosphopeptides associated with phosphoproteins of unknown functions were also detected. For example, a phosphopeptide NAVEDDAESDDEEVPEGR encoding an unknown phosphoprotein B4FQI5 was significantly increased in resistant maize Siyi after SCMV infection (Table 2). A phosphopeptide AGSGGPDTPVFGDR encoding an unknown phosphoprotein B6UBN4 was significantly decreased in susceptible Mo17 after SCMV infection (Table 1). Although they were previously annotated as phosphoproteins with unknown functions, they may be associated with new biological functions and may play important roles in plant-virus interactions.

Protein–protein interaction analysis

Generated networks reveal that some phosphoproteins which match the peptides with significantly altered phosphorylation levels by SCMV infection may interact with one another. Four major clusters, derived from the mapping of interologs from the phosphoproteins whose phosphorylation levels were significantly changed in susceptible maize Mo17 were associated with stress and metabolism process, photosynthesis, mRNA transcription and translation, and regulation of biological process (Fig. 5a, clusters AI, AII, AIII and AIV, respectively).

Cluster AI is composed of eight phosphoproteins: pyruvate orthophosphate dikinase, cytosolic orthophosphate dikinase, glucose-6-phosphate isomerase, phosphoglycerate kinase, fructose-6-phosphate-2-kinase/fructose-2, 6-bisphosphatase, nitrate reductase, carboxy-lyase and MAPK. These phosphoproteins are mainly involved in stress response and metabolism process. The second cluster (AII) contains phosphoproteins annotated to the photosynthesis system, including photosystem II reaction center protein and chlorophyll a/b-binding protein. The third cluster (AIII) consists of nine phosphoproteins, four of which are ribosomal proteins (two 40S ribosomal proteins, one 60S ribosomal protein, and one 60S acidic ribosomal protein),

indicating that translation is regulated and/or biased by phosphorylation. Another two phosphoproteins included in this cluster are arginine/serine-rich splicing factors. The remaining cluster (AIV) associated with biological process regulation and includes BZIP transcription factor, transposon protein mutator, and phototropic-responsive NPH3 family protein.

For the mapping of interologs from the phosphoproteins whose phosphorylation levels were significantly changed in resistant maize Siyi, four most connected clusters (clusters BI, BII, BIII and BIV) are shown in Fig. 5b. Cluster BI shares nine phosphoproteins, mainly involved in stress and defense response, including ferredoxin, phototropin, BZIP transcription factor and serine/threonine-protein kinase. The phosphoproteins interaction network of cluster BII was annotated to the regulation of biological process, in which MAPK was involved. For four phosphoproteins of cluster BIII, they were mainly involved in the biological processes "translation". Several phosphoproteins with evolutionarily conserved phosphorylation sites, which are involved in photosynthesis, showed close interactions and constitute the fourth cluster (BIV). Interactions among these phosphoproteins may play important roles in SCMV infection. In addition, the connectivity of the phosphoproteins in this biological network can also provide insight into their relative importance.

It should be noted that not all the phosphorylation changes in this study is biologically important. Promiscuous phosphorylation is a well-known phenomenon that occurs during in vitro assays since the concentration and location of reactants can be artificially high, thereby resulting in non-natural reactivity and phosphorylation patterns unreflective of true *in planta* chemistry (Kline et al. 2011). Furthermore, although a phosphosite is shown to change in vivo in response to stimuli, it does not mean that this site is biologically important. It is likely that a large number of phosphoproteins show dynamic phosphorylation status while only a few are necessary and/or sufficient for regulating a plant process (Kline et al. 2011). Therefore, to conclusively show that the phosphorylation change in this study is directly involved in SCMV infection, the forward or reverse genetics experiments are need to be performed in the future.

In summary, quantitative phosphoproteomic analysis of maize led to the identification of highly interesting key phosphoproteins involved in response to virus infection. The results of this study revealed overlapping and specific phosphoproteomic responses to SCMV infection between resistant and susceptible genotypes. Functions of the differentially regulated phosphoproteins in SCMV infection can be further tested using forward or reverse genetic approaches. It will also be very interesting to identify the kinases that phosphorylate these phosphoproteins in response to virus infection. In addition to providing a database of phosphopeptides and phosphoproteins that may involve in plant response to virus infection, our study has yielded new insights into molecular mechanism of plant-virus interactions.

Acknowledgments We thank Yingying Zhang for help with pathogen collection. This work was supported by the National Natural Science Foundation of China (31471503), the Ph.D Programs Foundation of the Ministry of Education of China (30600272) and the China Postdoctoral Science Foundation (201104369).

Conflict of interest We declare that we have no conflict of interest.

References

Arosio P, Levi S (2002) Ferritin, iron homeostasis, and oxidative damage. Free Radic Biol Med 33:457–463

Atkinson NJ, Urwin PE (2012) The interaction of plant biotic and abiotic stresses: from genes to the field. J Exp Bot 63:3523–3543

Baxter CJ, Foyer CH, Turner J, Rolfe SA, Quick WP (2003) Elevated sucrose-phosphate synthase activity in transgenic tobacco sustains photosynthesis in older leaves and alters development. J Exp Bot 54(389):1813–1820

Benschop JJ, Mohammed S, O'Flaherty M, Heck AJR, Slijper M, Menke FL (2007) Quantitative phosphoproteomics of early elicitor signaling in Arabidopsis. Mol Cell Proteomics 6:1198–1214

Bent AF (1996) Plant disease resistance genes: function meets structure. Plant Cell 8:1757–1771

Carroll AJ, Heazlewood JL, Ito J, Millar AH (2008) Analysis of the Arabidopsis cytosolic ribosome proteome provides detailed insights into its components and their post-translational modification. Mol Cell Proteomics 7:347–369

Cerny M, Dycka F, Bobál'ová J, Brzobohaty B (2011) Early cytokinin response proteins and phosphoproteins of Arabidopsis thaliana identified by proteome and phosphoproteome profiling. J Exp Bot 62:921–937

Christie JM (2007) Phototropin blue-light receptors. Annu Rev Plant Biol 58:21–45

Daniel JA, Yeager M (2005) Phosphorylation of aquaporin PvTIP3;1 defined by mass spectrometry and molecular modeling. Biochemistry 44:14443–14454

Di Carli M, Benvenuto E, Donini M (2012) Recent insight into plant-virus interactions through proteomic analysis. J Proteome Res 11:4765–4780

Escalante-Pérez M, Krol E, Stange A, Geiger D, Al-Rasheid KA, Hause B, Neher E, Hedrich R (2011) A special pair of phytohormones controls excitability, slow closure, and external stomach formation in the Venus flytrap. Proc Natl Acad Sci USA 108:15492–15497

Gan D, Zhang J, Jiang H, Jiang T, Zhu S, Cheng B (2010) Bacterially expressed dsRNA protects maize against SCMV infection. Plant Cell Rep 29:1261–1268

Gao B, Cui XW, Li XD, Zhang CQ, Miao HQ (2011) Complete genomic sequence analysis of a highly virulent isolate revealed a novel strain of Sugarcane mosaic virus. Virus Genes 43:390–397

Grimsrud PA, den Os D, Wenger CD, Swaney DL, Schwartz D, Sussman MR, Ané JM, Coon JJ (2010) Large-scale phosphoprotein analysis in Medicago truncatula roots provides insight into in vivo kinase activity in legumes. Plant Physiol 152:19–28

Gudesblat GE, Torres PS, Vojnov AA (2009) Stomata and pathogens: warfare at the gates. Plant Signal Behav 4(12):1114–1116

Hamel LP, Nicole MC, Sritubtim S, Morency MJ, Ellis M, Ehlting J, Beaudoin N, Barbazuk B, Klessig D, Lee J, Martin G, Mundy J, Ohashi Y, Scheel D, Sheen J, Xing T, Zhang S, Seguin A, Ellis BE (2006) Ancient signals: comparative genomics of plant MAPK and MAPKK gene families. Trends Plant Sci 11:192–198

Hanke GT, Kimata-Ariga Y, Taniguchi I, Hase T (2004) A post genomic characterization of Arabidopsis ferredoxins. Plant Physiol 134:255–2564

Huang HE, Ger MJ, Yip MK, Chen CY, Pandey AK, Feng TY (2004) A hypersensitive response was induced by virulent bacteria in transgenic tobacco plants overexpressing a plant ferredoxin-like protein (PFLP). Physiol Mol Plant Pathol 64:103–110

Huang C, Verrillo F, Renzone G, Arena S, Rocco M, Scaloni A, Marra M (2011) Response to biotic and oxidative stress in Arabidopsis thaliana: analysis of variably phosphorylated proteins. J Proteomics 74:1934–1949

Huber SC, Huber JLA (1996) Role and regulation of sucrosephosphate synthase in higher plants. Annu Rev Plant Physiol Plant Mol Biol 47:431–444

Kline KG, Barrett-Wilt GA, Sussman MR (2011) Quantitative Plant Phosphoproteomics. Curr Opin Plant Biol 14(5):507–511

Laporte MM, Galagon JA, Shapiro JA, Boersig MR, Shewmaker CR, Sharkey TD (2001) Promoter strength and tissue specificity effects on growth of tomato plants transformed with maize sucrose-phosphate synthase. Planta 212:817–822

Larsen MR, Thingholm TE, Jensen ON, Roepstorff P, Jørgensen TJ (2005) Highly selective enrichment of phosphorylated peptides from peptide mixtures using titanium dioxide microcolumns. Mol Cell Proteomics 4(7):873–886

Lasonder E, Green JL, Camarda G, Talabani H, Holder AA, Langsley G, Alano P (2012) The Plasmodium falciparum schizont phosphoproteome reveals extensive phosphatidylinositol and cAMP-protein kinase A signaling. J Proteome Res 11(11):5323–5337

Margaria P, Abbà S, Palmano S (2013) Novel aspects of grapevine response to phytoplasma infection investigated by a proteomic and phospho-proteomic approach with data integration into functional networks. BMC Genom 14:38

Maurel C (2007) Plant aquaporins: novel functions and regulation properties. FEBS Lett 581:2227–2236

Mehta A, Magalhães BS, Souza DS, Vasconcelos EA, Silva LP, Grossi-de-Sa MF, Franco OL, da Costa PH, Rocha TL (2008) Rooteomics: the challenge of discovering plant defense-related proteins in roots. Curr Protein Pept Sci 9:108–116

Morel JB, Dangl JL (1997) The hypersensitive response and the induction of cell death in plants. Cell Death Differ 4:671–683

Nakagami H, Sugiyama N, Mochida K, Daudi A, Yoshida Y, Toyoda T, Tomita M, Ishihama Y, Shirasu K (2010) Large-scale comparative phosphoproteomics identifies conserved phosphorylation sites in plants. Plant Physiol 153(3):1161–1174

Nguyen TH, Brechenmacher L, Aldrich JT, Clauss TR, Gritsenko MA et al (2012) Quantitative phosphoproteomic analysis of soybean root hairs inoculated with Bradyrhizobium japonicum. Mol Cell Proteomics 11(11):1140–1155

O'Rourke JA, Charlson DV, Gonzalez DO, Vodkin LO, Graham MA, Cianzio SR, Grusak MA, Shoemaker RC (2007) Microarray analysis of iron deficiency chlorosis in near-isogenic soybean lines. BMC Genom 8:476

Padhi A, Ramu K (2011) Genomic evidence of intraspecific recombination in sugarcane mosaic virus. Virus Genes 42:282–285

Pandey A, Mann M (2000) Proteomics to study genes and genomes. Nature 405:837–846

Perera MF, Filippone MP, Ramallo CJ, Cuenya MI, García ML, Ploper LD, Castagnaro AP (2009) Genetic diversity among viruses associated with sugarcane mosaic disease in Tucumán, Argentina. Phytopathology 99:38–49

Porra RJ, Thompson WA, Kriedemann PE (1989) Determination of accurate extinction coefficients and simultaneous equations for assaying chlorophyll a and b extracted with four different solvents: verification of the concentration of chlorophyll standards by atomic absorption spectroscopy. BBA Bioenergetics 975:384–394

Prak S, Hem S, Boudet J, Viennois G, Sommerer N, Rossignol M, Maurel C, Santoni V (2008) Multiple phosphorylations in the C-terminal tail of plant plasma membrane aquaporins. Mol Cell Proteomics 7:1019–1030

Roman DG, Dancis A, Anderson GJ, Klausner RD (1993) The fission yeast ferric reductase gene frp1 + is required for ferric iron uptake and encodes a protein that is homologous to the gp91-phox subunit of the human NADPH phagocyte oxidoreductase. Mol Cell Biol 13:4342–4350

Scharte J, Sch ÖH, Weis E (2005) Photosynthesis and carbohydrate metabolism in tobacco leaves during an incompatible interaction with Phytophthora nicotianae. Plant Cell Environ 28:1421–1435

Shin R, Alvarez S, Burch AY, Jez JM, Schachtman DP (2007) Phosphoproteomic identification of targets of the Arabidopsis sucrose nonfermenting-like kinase SnRK2.8 reveals a connection to metabolic processes. Proc Natl Acad Sci USA 104:6460–6465

Sinapidou E, Williams K, Nott L, Bahkt S, Tör M, Crute I, Bittner-Eddy P, Beynon J (2004) Two TIR:NB:LRR genes are required to specify resistance to Peronospora parasitica isolate Cala2 in Arabidopsis. Plant J 38:898–909

Stulemeijer IJ, Joosten MH, Jensen ON (2009) Quantitative phosphoproteomics of tomato mounting a hypersensitive response reveals a swift suppression of photosynthetic activity and a differential role for hsp90 isoforms. J Proteome Res 8(3):1168–1182

Sugiyama N, Nakagami H, Mochida K, Daudi A, Tomita M, Shirasu K, Ishihama Y (2008) Large-scale phosphorylation mapping reveals the extent of tyrosine phosphorylation in Arabidopsis. Mol Syst Biol 4:193. doi:10.1038/msb.2008.32

Taus T, Kocher T, Pichler P, Paschke C, Schmidt A, Henrich C, Mechtler K (2011) Universal and confident phosphorylation site localization using phosphors. J Proteome Res 10(12):5354–5362

van Loon L (1987) Disease induction by plant virus. Adv Virus Res 33:205–255

Viswanathan R, Karuppaiah R, Balamuralikrishnan M (2009) Identification of new variants of SCMV causing sugarcane mosaic in India and assessing their genetic diversity in relation to SCMV type strains. Virus Genes 39:375–386

Wiśniewski JR, Zougman A, Nagaraj N, Mann M (2009) Universal sample preparation method for proteome analysis. Nat Methods 6(5):359–362

Wu LJ, Zu XF, Wang SX, Chen YH (2012) Sugarcane mosaic virus—long history but still a threat to industry. Crop Prot 42:74–78

Wu LJ, Han ZP, Wang SX, Wang XT, Sun AG, Zu XF, Chen YH (2013) Comparative proteomic analysis of the plant–virus interaction in resistant and susceptible genotypes of maize infected with sugarcane mosaic virus. J Proteomics 89:124–140

Xing T, Laroche A (2011) Revealing plant defense signaling: getting more sophisticated with phosphoproteomics. Plant Signal Behav 6(10):1469–1474

Xu DL, Park JW, Mirkov TE, Zhou GH (2008) Viruses causing mosaic disease in sugarcane and their genetic diversity in southern China. Arch Virol 153:1031–1039

Zwerger K, Hirt H (2001) Recent advances in plant MAP kinase signalling. Biol Chem 382:1123–1131